White Matter Differences in Monozygotic Twins Discordant or Concordant for Obsessive-Compulsive Symptoms: A Combined Diffusion Tensor Imaging/Voxel-Based Morphometry Study

Anouk den Braber, Dennis van 't Ent, Dorret I. Boomsma, Danielle C. Cath, Dick J. Veltman, Paul M. Thompson, and Eco J.C. de Geus

Background: Neuroimaging studies of obsessive-compulsive disorder (OCD) patients point to deficits in cortico-striato-thalamo-cortical circuits that might include changes in white matter. The contribution of environmental and genetic factors to the various OCD-related changes in brain structures remains to be established.

Methods: White matter structures were analyzed in 140 subjects with both diffusion tensor imaging and voxel-based morphometry. We studied 20 monozygotic twin pairs discordant for obsessive-compulsive symptoms (OCS) to detect the effects of environmental risk factors for obsessive-compulsive (OC) symptomatology. Furthermore, we compared 28 monozygotic twin pairs concordant for low OCS scores with 23 twin pairs concordant for high OCS scores to detect the effects of genetic risk factors for OC symptomatology.

Results: Discordant pair analysis showed that the environmental risk was associated with an increase in dorsolateral-prefrontal white matter. Analysis of concordant pairs showed that the genetic risk was associated with a decrease in inferior frontal white matter. Various white matter tracts showed opposite effects of environmental and genetic risk factors (e.g., right medial frontal, left parietal, and right middle temporal), illustrating the need for designs that separate these classes of risk factors.

Conclusions: Different white matter regions were affected by environmental and genetic risk factors for OC symptomatology, but both classes of risk factors might, in aggregate, create an imbalance between the indirect loop of the cortico-striato-thalamo-cortical network (to the dorsolateral-prefrontal region)—important for inhibition and switching between behaviors—and the direct loop (involving the inferior frontal region) that contributes to the initiation and continuation of behaviors.

Obsessive-compulsive symptoms (OCS) have been defined as recurrent, persistent, and intrusive anxiety-provoking thoughts or images (obsessions) and subsequent repetitive behaviors (compulsions) performed to reduce anxiety and/or distress caused by the obsessions (1). When a person has these obsessions and/or performs compulsions for more than 1 hour/day and these thoughts and rituals significantly interfere with his/her daily life routines, the person fulfills the criteria for obsessive-compulsive disorder (OCD). OCD is generally assessed with structured clinical interviews (e.g., the Structured Clinical Interview for DSM Disorders [SCID]) (1). Additionally, questionnaires such as the Padua Inventory (2) and quantitative versions of the Yale-Brown Obsessive-Compulsive Scale (Y-BOCS) (3,4) might be used to rate OCS severity. The life-time prevalence of OCD is .5%–2% (1,5), but obsessions are much more prevalent in the general population—as high as 72% (6), and the prevalence of OCS reaches 20% (7).

Over the last 2 decades, neuroimaging studies have indicated several neurobiological changes underlying the psychological and behavioral deficits of OCD. Structural magnetic resonance imaging (MRI) has revealed regional volume differences in the ventral prefrontal cortex, dorsolateral prefrontal cortex (DLPFC), basal ganglia, anterior cingulate cortex, parietal cortex, and thalamus (8-14). Findings from functional neuroimaging studies are largely consistent with structural MRI findings and show altered regional activation in the aforementioned brain structures during performance of cognitive tasks and after symptom provocation (for a review, see [15]). Together, these findings contributed to the widely accepted neuroanatomical model of OCD involving the direct and indirect cortico–striato–thalamo– cortical (CSTC) loops (16,17). The direct loop functions as a self-reinforcing feedback loop that contributes to the initiation and continuation of behaviors. The indirect loop functions as a negative feedback loop important for inhibiting and switching between behaviors (17). It has been hypothesized that an imbalance between these loops, resulting in a hyperactive ventral and hypoactive dorsal frontal-striatal system, might mediate obsessive-compulsive (OC) symptomatology (16,17). Although a disturbance in these CSTC loops seems to be the neurological basis for OCD, several imaging studies suggest the involvement of other brain regions in OCD as well. For example, Menzies et al. (15) recently proposed an extended model that includes various brain areas (e.g., anterior cingulate cortex, amygdala, parietal areas) that are functionally connected to the direct and indirect loops.

So far, anatomical models of OCD have been mainly based on structural and functional MRI analyses that focused on gray matter differences in OCD patients compared with control subjects. More recent studies suggest an additional role for white matter abnormalities in the etiology of OCD (18-26), possibly related to variation

in genes involved in oligodendrocyte development (27). Diffusion tensor imaging (DTI) can be used to study white matter integrity, for instance in tracts that interconnect the brain regions of the CSTC loops. Diffusion tensor imaging provides a measure of diffusion of water molecules within tissues, permitting the investigation of brain tissue microstructure. In structures with a highly coherent directional organization (e.g., white matter tracts in the brain), the dominant direction of diffusion is parallel to the fiber direction, so that diffusion becomes more anisotropic (28-31). Fractional anisotropy (FA), a value that can be derived from diffusion tensor images, describes the degree of anisotropy within a voxel. Reduced FA might be interpreted as a reduced density of fibers, less directional coherence of fibers, or a reduced degree of myelination of fibers, all suggesting damaged or disorganized or underdeveloped white matter (28-31). To further investigate the nature of white matter alterations, T1-weighted scans can be analyzed with voxel-based morphometry (VBM). VBM, performed on white matter segmentations provides information on regional white matter volume differences (32,33). If an increase in FA is accompanied by an increase in white matter volume, the higher white matter integrity might indicate fibers that are more dense or more myelinated.

A few studies that used DTI to measure white matter abnormalities in OCD patients compared with healthy control subjects (18-26) have reported white matter differences near the caudate nucleus and thalamus (18,24), whereas others found differences predominantly in medial frontal and parietal regions (19,20,23). In addition, directly conflicting results were found, with reports of lower (19,23,25) and higher (18) FA in the left cingulate or no differences between patients and control subjects in this region at all (20). Such inconsistencies are usually explained as being due to methodological differences between studies, such as heterogeneity of patient groups and differences in sample size, scanning modalities/parameters, and analysis methods. However, there might also be "true" variability in the underlying neurobiology of OCD. That is, different white matter tract abnormalities might lead to comparable behavioral changes, because they occur in parts of the same brain network that regulates anxiety and safety behaviors. Such heterogeneity in affected white matter fibers might, in turn, reflect the differential influence of environmental and genetic risk factors for obsessive-compulsive (OC) symptomatology that might impact different parts of the brain (34).

Most clinical DTI studies employ standard case-control designs, comparing healthy control subjects with a group of affected individuals. These studies, however, cannot disentangle whether differences in brain white matter integrity are due to environmental versus genetic risk factors. One design that makes a distinction between environmentally and genetically mediated neurobiological differences that underlie the development of behavioral traits such as OCD is the discordant/concordant monozygotic (MZ) twin design (34-37). Nearly all MZ twins begin life with identical genomes, so behavioral discordances are likely to arise from differential exposure to environmental influences that can differentially modify gene expression in subjects with identical genotypes (38). Consequently, differences in central nervous system white matter between the high-risk twin and the low-risk co-twin reflect environmental effects on the brain rather than effects of genetic variation. To detect the effects of genetic risk factors, neuroimaging results can be compared between MZ twins who both score high for measures of OCS and MZ twins who both score very low for OCS. These MZ concordant high- and low-scoring twins are likely to come from families with either high or low vulnerability for OCD. Genetic epidemiological studies that compare MZ and dizygotic twin resemblance in OCS have already shown that the shared family environment does not influence these symptoms and that the familial vulnerability for this trait translates entirely to genetic vulnerability (39-41). Therefore, a comparison between MZ twins who both score high (concordant-high) for measures of OCS and MZ twins who both score low (concordant-low) for OCS can reveal white matter differences due to influences of genetic risk factors.

Our study aimed to examine the differential impact of non-shared environmental versus genetic influences on white matter regions in subjects at high risk for OCD. We compared DTI-derived FA maps between twins scoring low and twins scoring high on OCS from discordant MZ pairs and between concordant pairs where both twins scored either low or high on OCS. To confirm that an increase (decrease) in FA was accompanied by an increase (decrease) in white matter volume, we additionally examined white matter volumes in these specific regions with VBM.

Methods and Materials

Participants

The twin pairs included in this study were recruited from the Netherlands Twin Register (42). Surveys were sent to twin families, including the Padua Inventory Abbreviated (PI-R-ABBR) (43,44). Completed PI-R-ABBR questionnaires were returned by 815 MZ twin pairs (222 male; 593 female). From this sample we selected twin pairs in the age range between 18 and 60 years that scored discordant, concordant-high, or concordant-low for OCS. A twin pair was classified as discordant for OCS if one twin scored OCS high (> 16) and the co-twin scored OCS low (≤ 7). A twin pair was classified as concordant-high for OCS if both twins scored ≥ 15, with at least one twin scoring ≥ 16. A twin pair was classified as concordant-low for OCS if both twins scored ≤ 7. These PI-R-ABBR cutoff scores were derived from sensitivity and specificity measurements in a sample of OCD patients when compared with clinical control subjects ($n = 120$; mean scores 20.7, SD 8.1; sensitivity .74 and specificity .72 at the best cutoff point of 16 [43]). For more details on sample selection, we refer to den Braber *et al.* (34). A final sample of 71 MZ twin pairs participated in this MRI study, including 20 discordant, 23 concordant-high, and 28 concordant-low twin pairs (Table 1). The MRI protocol could not be completed by two subjects (metal artifact, panic attack). In the final sample ($n = 140$), two twins with high OCS scores from the discordant group and five twins with high OCS scores from the concordant-high group met clinical diagnosis for OCD. Furthermore, three twins with high OCS scores and one twin with a low OCS score from the discordant group and six twins from the concordant-high group used selective serotonin reuptake inhibitors (SSRIs).

Protocol

Participants were administered diagnostic interviews and questionnaires, including questions on demography, life-events, comorbidity, type and severity of OCS, tics, state-anger, and state anxiety (for a detailed description of the administered diagnostic interviews and questionnaires, please refer to den Braber *et al.* [34]). All twins were asked to collect mucosal cell samples for DNA extraction to test zygosity. The ethical review board of the VU University Medical Centre approved the study. All participants provided written informed consent.

Image Acquisition

The MRI session consisted of an anatomical scan of approximately 6 min and a DTI scan of approximately 3 min. During the scan sessions, the twins remained inside the scanner and were asked to minimize head movement during and between consecu-

Table 1. Twin Sample Demographic Data

	Twin Pairs							
	Discordant (Environmental Risk Measure)				Concordant (Genetic Risk Measure)			
	High (*n* = 20)	Low (*n* = 20)			High (*n* = 46)	Low (*n* = 56)		
Demographic Data								
Female	14				17	20		
Male	6				6	8		
Age, yrs (SD)	35.60 (8.68)				36.00 (10.55)	37.50 (8.79)		
	Mean (± SD)	Mean (± SD)	*t* Value	*p*	Mean (± SD)	Mean (± SD)	*t* Value	*p*
OCS								
PI-R-ABBR (0–48)	20.07 (5.03)	4.73 (1.84)	14.51	< .001	20.42 (4.56)	4.18 (2.19)	22.31	< .001
Y–BOCS severity lifetime (0–40)	7.70 (5.69)	6.70 (8.18)	.64	.527	10.41 (7.15)	3.18 (4.54)	5.13	< .001
Y–BOCS severity current (0–40)	5.45 (5.62)	1.45 (2.19)	3.64	.001	7.54 (5.83)	.95 (2.13)	6.95	< .001
Comorbidity								
MINI:								
Depression	2	0			0	0		
Panic disorder	1	0			0	0		
Agoraphobia	2	0			0	0		
Social disorder	1	0			2	0		
Posttraumatic stress disorder	1	0			0	0		
Generalized anxiety disorder	3	0			7	0		
Tic (0-8)	.40 (.75)	.20 (.41)	1.25	.214	.30 (.66)	.09 (.29)	2.03	.046
BDI (0–39)	4.65 (7.50)	3.05 (2.80)	1.73	.089	3.50 (3.17)	1.38 (2.18)	2.47	.016
STAI (0–60)	13.85 (8.54)	12.25 (6.13)	.83	.409	13.37 (7.39)	8.55 (7.36)	2.91	.005
STAS (0–30)	.20 (.70)	.00 (.00)	.91	.365	.46 (2.09)	.11 (.49)	1.09	.282

Values are given as (*n*), unless otherwise indicated. Twin pairs: number of female and male twin pairs; age: age at time of magnetic resonance imaging (MRI) examination (in years). OCS, obsessive-compulsive symptoms; PI-R-ABBR: mean Padua Inventory Abbreviated Scores (SD); Y–BOCS severity lifetime/current: mean Yale–Brown Obsessive–Compulsive Scale severity scores (SD) across whole life span and at the time of MRI; MINI (depression, panic disorder, agoraphobia, social disorder, posttraumatic stress disorder, generalized anxiety disorder): number of subjects with current comorbid disorder (measured with the Mini International Neuropsychiatric Interview); Tic: mean Tic scores (SD) at time of MRI; BDI: mean Beck Depression Inventory scores (SD) at time of MRI; STAI: mean State Trait Anxiety Inventory scores (SD) at time of MRI; STAS: mean State Trait Anger Scale scores (SD) at time of MRI.

tive runs. To reduce motion artifacts, the head of each participant was immobilized with foam pads.

MRI was performed on a 3.0 T Intera MR system (Philips Medical Systems, Best, the Netherlands) with a standard SENSE receiver head coil. The anatomical scan consisted of 182 coronal slices with a three-dimensional T1-weighted gradient-echo sequence (flip angle 8°; repetition time = 9.69 msec; echo time = 4.60 msec; matrix, 256 × 256 pixels; voxel size, 1.00 × 1.00 × 1.20 mm). Diffusion tensor images were obtained in 32 directions with single-shot echoplanar acquisition (flip angle 90°; repetition time = 4834 msec; echo time = 94 msec; matrix, 112 × 110 pixels; voxel size, 2.00 × 2.00 × 3.00 mm; b-value 1000 sec/mm^2, 38 axial slices).

Data Analysis

The FA maps were calculated from raw DTI scans with the Medical Image Navigation and Research Tool by INRIA (MEDINRIA, Asclepios Research Project—INRIA Sophia Antipolis, France). The MRI data were further analyzed with SPM8 (Wellcome Department of Imaging Neuroscience, London, United Kingdom). T1-weighted magnetic resonance images were segmented into gray matter, white matter, and cerebrospinal fluid and normalized to a group template (i.e., a specific template for the discordant and concordant twins) with the Diffeomorphic Anatomical Registration Through Exponential Lie algebra (DARTEL) algorithm, and subsequently warped from DARTEL space to the standard Montreal Neurological Institute brain. The FA maps were first coregistered with T1-

weighted magnetic resonance images and normalized with each subject's T1 to DARTEL to Montreal Neurological Institute warp parameters. Subsequently, data were spatially smoothed with an 8-mm isotropic Gaussian kernel.

Statistical Tests

Differences in survey- and interview-based variables were tested with a mixed-model analysis of variance (Mixed Models Linear menu item in SPSS; SPSS, Chicago, Illinois) with twin pair type (discordant vs. concordant) and OCS score level (high vs. low) as two fixed factors and family as a random factor to account for within-twin pair dependence. Statistical results were considered significant at *p* < .05, Bonferroni corrected.

Differences in FA maps between OCS high- and OCS low-scoring twins from discordant pairs were investigated with a paired sample *t* test. Differences in FA maps between concordant OCS high and concordant OCS low twin pairs were assessed with an analysis of variance group comparison. To account for within-twin pair correlations, FA maps of the twin and co-twin of each concordant pair were entered as repeated measures. Group differences are reported at an uncorrected individual voxel threshold of *p* < .005, with a minimal cluster extent of 50 voxels, which is slightly more conservative as used in previous DTI studies of OCD (18,23,25).

To test whether an increase (decrease) in FA is accompanied by an increase (decrease) in white matter volume, an additional region of interest (ROI) analysis was performed on the structural VBM data.

That is, we tested for increased (decreased) white matter volumes in the discordant and concordant structural data specifically in spherical ROIs (radius 10 mm) centered on the coordinates where discordant and concordant pairs showed maximally increased (decreased) FA. For these post hoc ROI analyses, an individual voxel *p* value threshold of *p* < .05 was applied, corrected for multiple comparisons (family-wise error).

Results

Questionnaire and Interview Data

As expected, OCS high- compared with low-scoring twins in both the discordant and concordant groups showed significant higher scores on the PI-R-ABBR and current Y–BOCS severity scale (Table 1). In addition, high-scoring twins were more often diagnosed with current comorbid disorders, which were absent in the low-scoring twins.

Environmental Risk: OCS High Versus Low Scoring Twins from Discordant Pairs

DTI—FA. Figure 1 and Table 2A summarize the FA results of the OCS high versus low within twin pair comparison of the discordant pairs. Relative to their low-scoring co-twins, OCS high-scoring twins exhibited clusters of increased FA in right orbitofrontal (cluster label A in Table 2A and Figure 1), left dorsolateral prefrontal (cluster label B), left precentral (cluster label C), left corpus callosum (cluster label D), left cingulate (cluster label E), left insula (cluster label F), right superior parietal (cluster label G), and right temporal (cluster label H) regions and bilaterally in cerebellar regions (cluster labels I and J). Clusters of decreased FA in OCS high-

compared with their low-scoring co-twins were observed bilaterally in medial frontal and temporal regions (cluster labels K, L, N, P, and Q in Table 2A and Figure 1), right insula (cluster label M), left parietal (cluster label O), and right occipital (cluster label R) regions and left brainstem/pons (cluster label S).

Structural VBM Data—ROI Analysis. An ROI analysis of the structural VBM data at coordinates that showed maximal within-pair differences in FA in the discordant sample revealed a significant increase in white matter volume in the left DLPFC. Furthermore, a trend toward decreased white matter volumes in the high- compared with low-scoring twins was found in the right medial frontal and left parietal cortex (Table 2B and indicated *Z* scores in Figure 1).

Genetic Risk: Concordant High- Versus Concordant Low-Scoring Twins

DTI—FA. Table 3A and Figure 2 show clusters of OCS-related FA differences between the concordant-high and -low twin pairs. Concordant-high-scoring twins compared with OCS low-scoring twins exhibited clusters of increased FA in right medial frontal (cluster label T in Table 3A and Figure 2) and right temporal (cluster label W) regions and bilaterally in parietal regions (cluster label U and V). A cluster of decreased FA in OCS high- compared with low-scoring twins was observed in the left inferior frontal lobe (cluster label X in Table 3A and Figure 2).

Structural VBM Data—ROI Analysis. An ROI analysis of the structural VBM data at coordinates that showed maximal between-group differences in FA in the concordant sample revealed a significant decrease in white matter volume in the high compared with
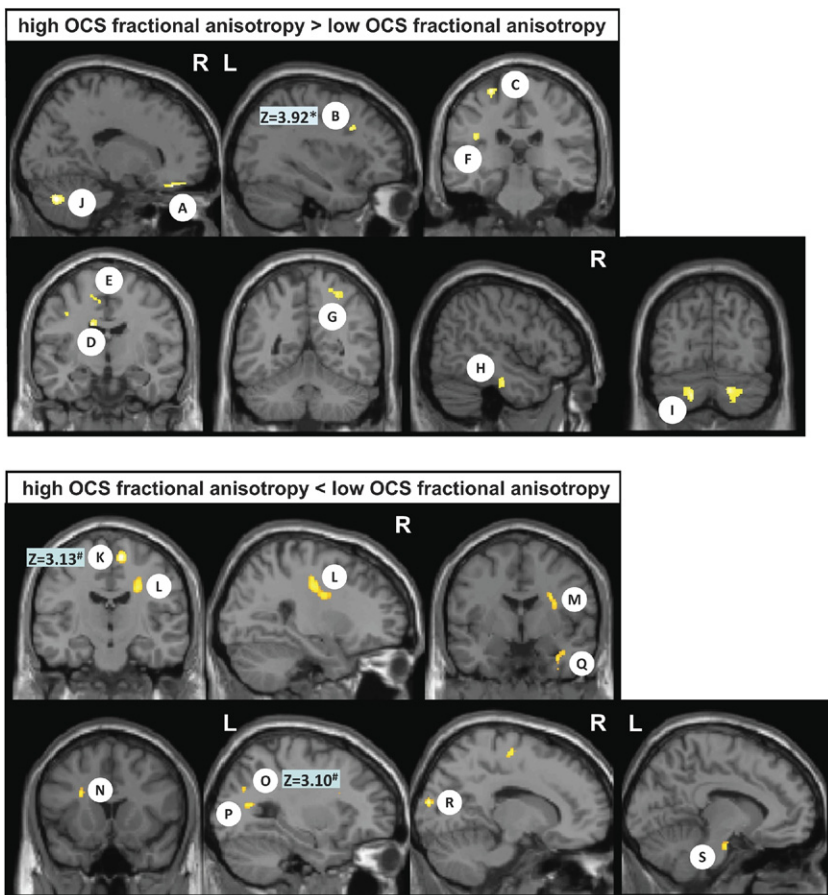

Figure 1. Environmental risk: fractional anisotropy (FA) in high obsessive-compulsive symptoms (OCS) relative to low OCS discordant twins. Brain regions showing increased (top panels: high > low) and reduced (bottom panels: high < low) FA in OCS high vs. low twins of the discordant sample. Z: *z* value of voxel with largest effect size derived from additional voxel-based morphometry–region-of-interest analysis, *p < .05, family-wise error (FWE)-corrected; #trend toward *p* < .05, FWE-corrected.

Table 2. Environmental Risk: Regional White Matter Differences Between OCS High and Low Twins of the Discordant Sample

	Regional White Matter FA Within-Pair Differences[a]							Regional White Matter Volume Within-Pair Differences[b]					
	MNI Coordinates			Z Score	p Value	Voxels (n)	Anatomical Location	Cluster Label	MNI Coordinates (ROI VBM)			t Value	p Value	Voxels (n)
Test	x	y	z						x	y	z			
High > Low	18	39	−23	3.6	< .001	98	right orbitofrontal	A	—	—	—	—	—	—
	−34	15	31	3.19	.001	57	left dorsolateral prefrontal	B	−25	14	31	4.94	.008[c]	194
	−25	−27	66	3.46	< .001	65	left precentral	C	—	—	—	—	—	—
	−13	−10	27	3.63	< .001	189	left corpus callosum	D	—	—	—	—	—	—
	−13	−7	63	3.31	< .001	81	left cingulate	E	—	—	—	—	—	—
	−41	−30	21	3.37	< .001	101	left insula	F	—	—	—	—	—	—
	29	−51	57	3.16	.001	69	right superior parietal	G	—	—	—	—	—	—
	48	−16	−26	3.08	.001	50	right temporal	H	—	—	—	—	—	—
	−17	−73	−39	3.34	< .001	295	left cerebellum, pyramis/tonsil	I	—	—	—	—	—	—
	20	−70	−35	3.67	< .001	488	right cerebellum, uvula/pyramis	J	—	—	—	—	—	—
High < Low	11	−15	63	4.23	< .001	167	right medial frontal	K	11	−18	68	3.63	.075[d]	88
	27	−15	36	3.6	< .001	551	right medial frontal	L	—	—	—	—	—	—
	32	2	15	3.36	< .001		right insula	M	—	—	—	—	—	—
	−25	15	24	3.12	.001	128	left medial frontal	N	—	—	—	—	—	—
	−33	−67	32	3.35	< .001	50	left parietal	O	−28	−61	26	3.59	.081[d]	33
	−28	−67	12	3.24	.001	53	left temporal	P	—	—	—	—	—	—
	35	−6	−30	4.08	< .001	128	right middle temporal	Q	—	—	—	—	—	—
	15	−91	17	3.92	< .001	91	right occipital	R	—	—	—	—	—	—
	−9	−12	−27	3.27	.001	64	left brainstem, pons	S	—	—	—	—	—	—

MNI, Montreal Neurological Institute; VBM, voxel-based morphometry; other abbreviations as in Table 1.

[a]Clusters with regional fractional anisotropy (FA) differences between OCS high and low twins in the discordant sample. Test: test for significant FA increases (high > low) or decreases (high < low) in OCS high- relative to OCS low-scoring twins; MNI coordinates (mm): location of voxel with largest effect size; Z score: z value of voxel with largest effect size; p value: cluster p value; Voxels (n): number of voxels in cluster; cluster label: alphabetical cluster label as displayed in anatomical overlays of Figure 1.

[b]Clusters with regional white matter volume differences between OCS high and low twins in the discordant sample in spherical region of interest (ROIs) (radius 10 mm) centered on the coordinates where discordant pairs showed maximally increased (decreased) FA. MNI coordinates (mm): location of voxel with largest effect size; p value: cluster p value family-wise error (FWE)-corrected; voxels (n): number of voxels in cluster.

[c]$p < .05$, FWE-corrected.

[d]Trend toward $p < .05$, FWE-corrected.

low concordant twins in the left inferior frontal lobe. No clusters of increased white matter volumes were found (Table 3B and indicated Z scores in Figure 2).

Because this study included subjects with SSRI medication, we conducted additional analyses to test whether removing these subjects from the analyses would affect the results. We re-ran the analysis on 17 discordant pairs and 20 concordant-high versus 28 concordant-low pairs not taking SSRIs. These analyses did not affect the pattern of results.

Discussion

White matter structures were compared with a combined DTI-VBM analysis within MZ twin pairs discordant for OCS and between MZ twin pairs concordant-low or concordant-high for OCS. Discordant pair analysis indicated that environmental risk factors for OC symptomatology were associated with increases in dorsolateral prefrontal white matter. Concordant pairs analysis suggested that genetic risk factors for OC symptomatology were associated with decreases in inferior frontal white matter. Remarkably, DTI analysis indicated that some white matter tracts show FA alterations that are in the opposite direction in subjects at high environmental risk compared with subjects at high genetic risk (e.g., right medial fron-

tal, left parietal, and right middle temporal). Results are discussed in more detail in the following text, in which we focus on the areas that were detected by DTI and confirmed by the VBM analysis. VBM not only shows that the white matter differences identified by DTI indicate a change in the number of fibers or higher degree of myelination of fibers; it also provides a within-study replication of white matter abnormalities by a different method.

Environmentally Mediated White Matter Alterations

The dorsolateral prefrontal region showed increased white matter integrity (FA), accompanied by increased white matter volume (VBM), in OCS high- compared with OCS low-scoring twins only in the discordant sample. Thus, these white matter differences are likely related to environmental risk factors for OC symptomatology. An increased FA in the dorsolateral prefrontal region, as found in subjects at high environmental risk for OCD, was also found by Ha *et al.* (19) and is in line with literature in OCD (15). The DLPFC has been related to executive processing, including attention, response inhibition, cognitive planning, and decision making (45-47). Neuropsychological studies have typically associated dysfunction of the DLPFC with perseverative, disinhibited behaviors, which OCD patients particularly show during the completion of their compulsions

Table 3. Genetic Risk: Regional White Matter Differences Between OCS High and Low Twins of the Concordant Sample

Regional White Matter FA Between-Group Differences[a]									Regional White Matter Volume Between-Group Differences[b]					
	MNI Coordinates			Z		Voxels	Anatomical	Cluster	MNI Coordinates (ROI VBM)					Voxels
Test	x	z	y	Score	p Value	(n)	Location	Label	x	y	z	t Value	p Value	(n)
High > Low	14	−13	56	3.41	< .001	78	right medial frontal	T	—	—	—	—	—	—
	−21	−48	38	3.22	.001	142	left parietal	U	—	—	—	—	—	—
	29	−43	36	3.08	.001	51	right parietal	V	—	—	—	—	—	—
	39	0	−24	3.40	< .001	86	right middle temporal	W	—	—	—	—	—	—
High < Low	−51	27	3	3.99	< .001	166	left inferior frontal	X	−46	27	1	3.03	.047[c]	41

[a]Cluster with regional FA differences between concordant-high and low twins. Test: test for significant FA increases (high > low) or decreases (high < low) in OCS high- relative to OCS low-scoring twins; MNI coordinates (mm): location of voxel with largest effect size; Z score: z value of voxel with largest effect size; p value: cluster p value; voxels (n): number of voxels in cluster; cluster label: alphabetical cluster label as displayed in anatomical overlays of Figure 2.

[b]Clusters with regional white matter volume differences between OCS high and low twins in the concordant sample in spherical ROIs (radius 10 mm) centered on the coordinates where concordant pairs showed maximally increased (decreased) FA. MNI coordinates (mm): location of voxel with largest effect size; p value: cluster p value FWE-corrected; voxels (n): number of voxels in cluster. Abbreviations as in Table 2.

[c]$p < .05$, FWE-corrected.

(48). The finding of systematic differences in white matter integrity in the DLPFC is consistent with the commonly accepted neurobiological model of CSTC abnormalities in OCD (49,50). In addition, this region was also implicated in OCD by a previous functional MRI study by our group that showed an environmentally mediated decrease in DLPFC activity during the performance of a Tower of London planning paradigm (34).

Some white matter regions showed altered FA in high compared with low discordant twins that were not corroborated by our VBM-ROI analysis but replicate previous DTI findings in OCD patients. These include the corpus callosum and the cingulate bundle (18,24,25). An environmentally mediated increase in FA was found in the body of the corpus callosum, which interconnects motor and posterior parietal regions (22). This is in line with results from a morphological study that found significantly larger corpus callosal areas in pediatric OCD patients compared with control subjects

Figure 2. Genetic risk: FA in high OCS relative to low OCS concordant twins. Brain regions showing increased (top panels: high > low) and reduced (bottom panels: high < low) FA in concordant-high vs. concordant-low twins. Z: z value of voxel with largest effect size derived from additional voxel-based morphometry–region-of-interest analysis, *p < .05, FWE-corrected. Abbreviations as in Figure 1.

(51). The cingulate bundle is one of the main white matter tracts that connects the gray matter nodes of the neural circuitry implicated in OCD (52,53). We found FA was higher in the cingulate bundle in the discordant OCS high twins, which replicates the finding by Cannistraro *et al.* (18) in patients with OCD compared with healthy control subjects. The cingulate effect might be specific to environmental risk factors, because Menzies *et al.* (20), who performed a ROI analysis in OCD patients and their first-degree relatives, did not find FA alterations in the cingulate bundle in either patients or their first-degree relatives.

Genetically Mediated White Matter Alterations

The inferior frontal region showed lower white matter integrity (FA), accompanied by decreased white matter volume (VBM) in OCS high- compared with OCS low-scoring twins only in the concordant sample. These white matter deficits are likely related to genetic risk factors for OC symptomatology. The inferior frontal region is also implicated in the widely accepted neuroanatomical CSTC model for OCD and is involved in a wide range of cognitive processes, including task switching, reversal learning, and cognitive and emotional inhibition (54,55). Furthermore, this region is involved in regulating socially appropriate behaviors, and when impaired a person might show impulsive and disinhibited behavior (48). In addition, this region was also implicated in a previous functional study by our group that showed a genetically mediated increase in inferior frontal activity during the performance of a Tower of London planning paradigm (34).

White Matter Changes Related to Both Environmental and Genetic Risk Factors

Regions that showed FA alterations in both the discordant and concordant sample include medial frontal, parietal, and temporal regions. Interestingly, if we examine our results in more detail, roughly the same white matter regions show FA alterations, but these are in the opposite direction (increased vs. decreased) in subjects at high environmental risk compared with subjects at high genetic risk (e.g., right medial frontal: reduced FA in discordants, increased FA in concordants; left parietal: reduced FA in discordants, increased FA in concordants; right temporal: reduced FA in discordants, increased FA in concordants). This pattern of opposite DTI findings for the same anatomical region echoes a similar disparity in the extant literature. For instance, some studies found de-
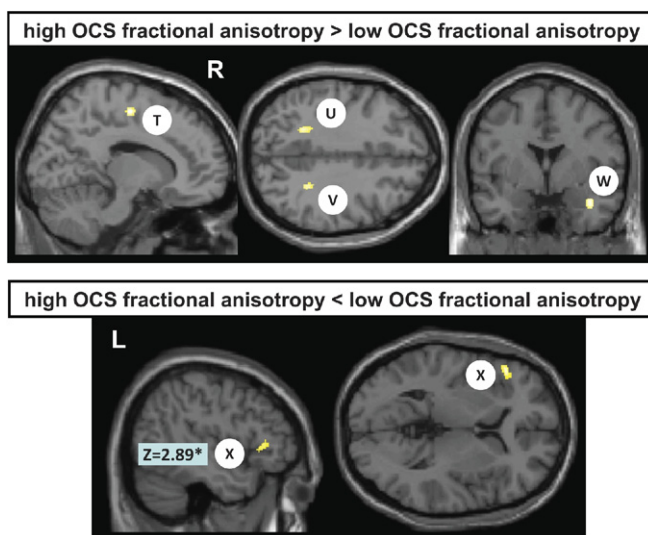
creased FA in the corpus callosum in patients with OCD compared with control subjects (22,25), whereas others reported increased FA in OCD patients for this region (24). This pattern of findings makes most sense when we allow environmental and genetic risk factors to affect the brain in different ways. This is, in fact, a major rationale to apply the discordant/concordant twin design.

Patient samples represent an unknown mixture of individuals who developed OCD due to a genetic predisposition and/or environmental triggers. Our results illustrate that, if the study sample predominantly consists of patients with a familial predisposition, findings might differ from those of a study of patients who might have developed the disorder due to a negative environmental experience (e.g., divorce, sexual assault). A previous study attempting to identify genetic markers for OCD by comparing FA alterations in OCD patients, their first-degree relatives, and control subjects found an FA increase in right medial frontal white matter (20). This result is in line with our finding of a genetically mediated FA increase in the same region, which might indicate that this alteration is specific to individuals at increased genetic risk for OCD. However, this finding could be easily missed if a sample represents a mixture of subjects at increased genetic risk and subjects with environmentally mediated OCD. This might be true of the various studies that failed to find FA alterations in this region (18,24,25). Medial frontal,

parietal, and temporal regions have been implicated in the neuroanatomical model for OCD, predominantly through their functional connections with the ventral prefrontal cortex and DLPFC. An alteration in these functional connections might lead to an imbalance between the direct and indirect pathways, which subsequently might induce OC-like behavior.

To summarize, inconsistencies between results of previously performed imaging studies might be related, at least in part, to "true" variability in the underlying neurobiology of OCD. The present results suggest that the effects on central nervous system white matter regions of environmental risk factors for OC symptomatology are distinct from those of the genetic risk for OC symptomatology. These findings are in line with results from a previous functional imaging study by our group (34) in which these same regions were found to be differentially affected by environmental and genetic risk factors for OC symptomatology. Interestingly, when the DTI-VBM and functional MRI results are taken together, they point toward an inverse relation between task-related activity and white matter integrity in OCS (e.g., environmentally mediated decrease in DLPFC activity coupled with higher dorsolateral prefrontal white matter integrity, and genetically mediated increase in inferior frontal activity together with lower inferior frontal white matter integrity). This inverse relation might be the result of an increase or
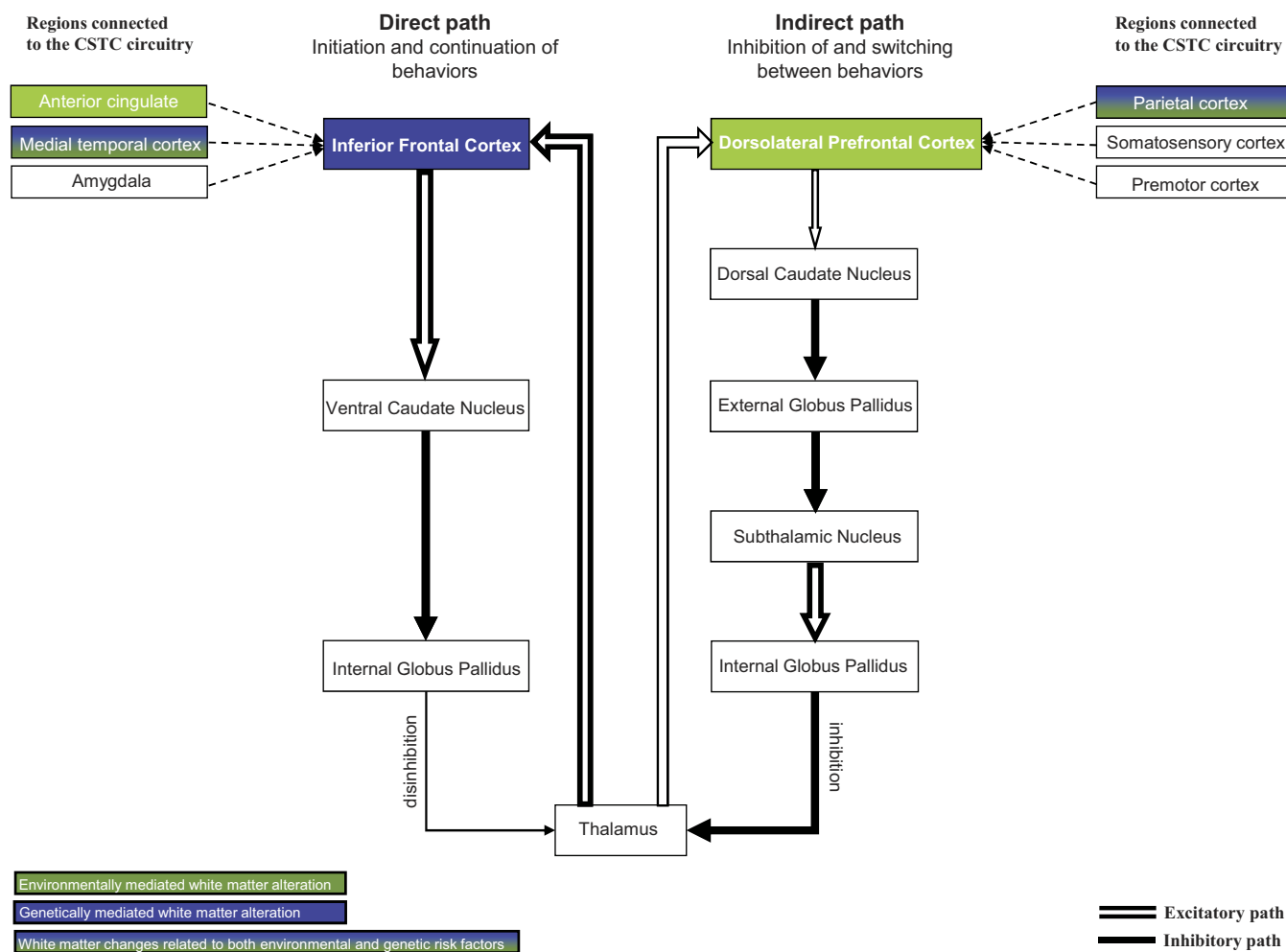

Figure 3. Model illustrating distinct genetically and environmentally mediated white matter alterations as suggested by the present study implemented in the widely accepted neurobiological model for obsessive-compulsive disorder, suggesting an imbalance between the indirect and direct path (adapted from Menzies *et al.* [15] and Mataix-Cols *et al.* [17]). CSTC, cortico–striato–thalamo–cortical.

A. den Braber *et al.*

decrease, respectively, in inhibitory signaling in these specific regions that depends on white matter integrity.

Although different regions seemed to be affected by environmental and genetic risk factors for OC symptomatology, both classes of risk factors strikingly converge on the CSTC loops. Neurobiological changes in OCS induced by environmental risk factors involve the indirect loop of the CSTC (dorsolateral prefrontal region), which functions as a negative feedback loop important for the inhibition of and switching between behaviors. By contrast, neurobiological changes in OCS induced by genetic risk factors involve regions implicated in the direct loop of the CSTC (inferior frontal region), which functions as a self-reinforcing feedback loop that contributes to the initiation and continuation of behaviors (Figure 3).

1. American Psychiatric Association (1994): *Diagnostic and Statistical Manual of Mental Disorder, 4th Edition*. Washington, DC: American Psychiatric Association.
2. Sanavio E (1988): Obsessions and compulsions: The Padua Inventory. *Behav Res Ther* 26:169–177.
3. Goodman WK, Price LH, Rasmussen SA, Mazure C, Delgado P, Heninger GR, *et al.* (1989): The Yale-Brown Obsessive Compulsive Scale. II. Validity. *Arch Gen Psychiatry* 46:1012–1016.
4. Goodman WK, Price LH, Rasmussen SA, Mazure C, Fleischmann RL, Hill CL, *et al.* (1989): The Yale-Brown Obsessive Compulsive Scale. I. Development, use, and reliability. *Arch Gen Psychiatry* 46:1006–1011.
5. Grabe HJ, Meyer C, Hapke U, Rumpf HJ, Freyberger HJ, Dilling H, *et al.* (2000): Prevalence, quality of life and psychosocial function in obsessive-compulsive disorder and subclinical obsessive-compulsive disorder in northern Germany. *Eur Arch Psychiatry Clin Neurosci* 250:262–268.
6. Rachman S, de Silva P (1978): Abnormal and normal obsessions. *Behav Res Ther* 16:233–248.
7. Fullana MA, Mataix-Cols D, Caspi A, Harrington H, Grisham JR, Moffitt TE, *et al.* (2009): Obsessions and compulsions in the community: Prevalence, interference, help-seeking, developmental stability, and co-occurring psychiatric conditions. *Am J Psychiatry* 166:329–336.
8. Pujol J, Soriano-Mas C, Alonso P, Cardoner N, Menchon JM, Deus J, Vallejo J (2004): Mapping structural brain alterations in obsessive-compulsive disorder. *Arch Gen Psychiatry* 61:720–730.
9. Valente AA Jr, Miguel EC, Castro CC, Amaro E Jr, Duran FL, Buchpiguel CA, *et al.* (2005): Regional gray matter abnormalities in obsessive-compulsive disorder: A voxel-based morphometry study. *Biol Psychiatry* 58:479–487.
10. van den Heuvel OA, Remijnse PL, Mataix-Cols D, Vrenken H, Groenewegen HJ, Uylings HB, *et al.* (2009): The major symptom dimensions of obsessive-compulsive disorder are mediated by partially distinct neural systems. *Brain* 132:853–868.
11. Rotge JY, Guehl D, Dilharreguy B, Tignol J, Bioulac B, Allard M, *et al.* (2009): Meta-analysis of brain volume changes in obsessive-compulsive disorder. *Biol Psychiatry* 65:75–83.
12. Menzies L, Achard S, Chamberlain SR, Fineberg N, Chen CH, Del Campo N, *et al.* (2007): Neurocognitive endophenotypes of obsessive-compulsive disorder. *Brain* 130:3223–3236.
13. Radua J, Mataix-Cols D (2009): Voxel-wise meta-analysis of grey matter changes in obsessive-compulsive disorder. *Br J Psychiatry* 195:393–402.
14. Radua J, van den Heuvel OA, Surguladze S, Mataix-Cols D (2010): Meta-analytical comparison of voxel-based morphometry studies in obsessive-compulsive disorder vs other anxiety disorders. *Arch Gen Psychiatry* 67:701–711.
15. Menzies L, Chamberlain SR, Laird AR, Thelen SM, Sahakian BJ, Bullmore ET (2008): Integrating evidence from neuroimaging and neuropsychological

16. Saxena S, Rauch SL (2000): Functional neuroimaging and the neuroanatomy of obsessive-compulsive disorder. *Psychiatr Clin North Am* 23:563–586.
17. Mataix-Cols D, van den Heuvel OA (2006): Common and distinct neural correlates of obsessive-compulsive and related disorders. *Psychiatr Clin North Am* 29:391–410, viii.
18. Cannistraro PA, Makris N, Howard JD, Wedig MM, Hodge SM, Wilhelm S, *et al.* (2006): A diffusion tensor imaging study of white matter in obsessive-compulsive disorder. *Depress Anxiety* 24:440–446.
19. Ha TH, Kang DH, Park JS, Jang JH, Jung WH, Choi JS, *et al.* (2009): White matter alterations in male patients with obsessive-compulsive disorder. *Neuroreport* 20:735–739.
20. Menzies L, Williams GB, Chamberlain SR, Ooi C, Fineberg N, Suckling J, *et al.* (2008): White matter abnormalities in patients with obsessive-compulsive disorder and their first-degree relatives. *Am J Psychiatry* 165:1308–1315.
21. Nakamae T, Narumoto J, Shibata K, Matsumoto R, Kitabayashi Y, Yoshida T, *et al.* (2008): Alteration of fractional anisotropy and apparent diffusion coefficient in obsessive-compulsive disorder: A diffusion tensor imaging study. *Prog Neuropsychopharmacol Biol Psychiatry* 32:1221–1226.
22. Saito Y, Nobuhara K, Okugawa G, Takase K, Sugimoto T, Horiuchi M, *et al.* (2008): Corpus callosum in patients with obsessive-compulsive disorder: Diffusion-tensor imaging study. *Radiology* 246:536–542.
23. Szeszko PR, Ardekani BA, Ashtari M, Malhotra AK, Robinson DG, Bilder RM, *et al.* (2005): White matter abnormalities in obsessive-compulsive disorder: A diffusion tensor imaging study. *Arch Gen Psychiatry* 62:782–790.
24. Yoo SY, Jang JH, Shin YW, Kim DJ, Park HJ, Moon WJ, *et al.* (2007): White matter abnormalities in drug-naive patients with obsessive-compulsive disorder: A diffusion tensor study before and after citalopram treatment. *Acta Psychiatr Scand* 116:211–219.
25. Garibotto V, Scifo P, Gorini A, Alonso CR, Brambati S, Bellodi L, *et al.* (2010): Disorganization of anatomical connectivity in obsessive-compulsive disorder: A multi-parameter diffusion tensor imaging study in a subpopulation of patients. *Neurobiol Dis* 37:468–476.
26. Nakamae T, Narumoto J, Sakai Y, Nishida S, Yamada K, Nishimura T, *et al.* (2010): Diffusion tensor imaging and tract-based spatial statistics in obsessive-compulsive disorder. *J Psychiatr Res* 45:687–690.
27. Stewart SE, Platko J, Fagerness J, Birns J, Jenike E, Smoller JW, *et al.* (2007): A genetic family-based association study of OLIG2 in obsessive-compulsive disorder. *Arch Gen Psychiatry* 64:209–214.
28. Mori S, Zhang J (2006): Principles of diffusion tensor imaging and its applications to basic neuroscience research. *Neuron* 51:527–539.
29. Beaulieu C (2002): The basis of anisotropic water diffusion in the nervous system—a technical review. *NMR Biomed* 15:435–455.
30. Basser PJ, Pierpaoli C (1996): Microstructural and physiological features of tissues elucidated by quantitative-diffusion-tensor MRI. *J Magn Reson B* 111:209–219.
31. Le Bihan D, Mangin JF, Poupon C, Clark CA, Pappata S, Molko N, *et al.* (2001): Diffusion tensor imaging: Concepts and applications. *J Magn Reson Imaging* 13:534–546.
32. Ashburner J, Friston KJ (2000): Voxel-based morphometry—the methods. *Neuroimage* 11:805–821.
33. Ashburner J, Friston KJ (2001): Why voxel-based morphometry should be used. *Neuroimage* 14:1238–1243.
34. den Braber A, van 't Ent D, Cath DC, Wagner J, Boomsma DI, de Geus EJC (2010): Brain activation during cognitive planning in twins discordant or concordant for obsessive-compulsive symptoms. *Brain* 133:3123–3140.
35. de Geus EJ, van 't Ent D, Wolfensberger SP, Heutink P, Hoogendijk WJ, Boomsma DI, *et al.* (2007): Intrapair differences in hippocampal volume in monozygotic twins discordant for the risk for anxiety and depression. *Biol Psychiatry* 61:1062–1071.
36. van 't Ent D, van Beijsterveldt TC, Derks EM, Hudziak JJ, Veltman DJ, Todd RD, *et al.* (2009): Neuroimaging of response interference in twins concordant or discordant for inattention and hyperactivity symptoms. *Neuroscience* 164:16–29.
37. Wolfensberger SP, Veltman DJ, Hoogendijk WJ, Boomsma DI, de Geus EJ (2008): Amygdala responses to emotional faces in twins discordant or concordant for the risk for anxiety and depression. *Neuroimage* 41:544–552.

38. Heijmans BT, Tobi EW, Lumey LH, Slagboom PE (2009): The epigenome: Archive of the prenatal environment. *Epigenetics* 4:526–531.

39. van Grootheest DS, Cath DC, Beekman AT, Boomsma DI (2007): Genetic and environmental influences on obsessive-compulsive symptoms in adults: A population-based twin-family study. *Psychol Med* 37:1635–1644.

40. Jonnal AH, Gardner CO, Prescott CA, Kendler KS (2000): Obsessive and compulsive symptoms in a general population sample of female twins. *Am J Med Genet* 96:791–796.

41. Clifford CA, Murray RM, Fulker DW (1984): Genetic and environmental influences on obsessional traits and symptoms. *Psychol Med* 14:791–800.

42. Boomsma DI, de Geus EJ, Vink JM, Stubbe JH, Distel MA, Hottenga JJ, *et al.* (2006): Netherlands Twin Register: From twins to twin families. *Twin Res Hum Genet* 9:849–857.

43. Cath DC, van Grootheest DS, Willemsen G, van Oppen P, Boomsma DI (2008): Environmental factors in obsessive-compulsive behavior: Evidence from discordant and concordant monozygotic twins. *Behav Genet* 38:108–120.

44. van Oppen P, Hoekstra RJ, Emmelkamp PM (1995): The structure of obsessive-compulsive symptoms. *Behav Res Ther* 33:15–23.

45. Faw B (2003): Pre-frontal executive committee for perception, working memory, attention, long-term memory, motor control, and thinking: A tutorial review. *Conscious Cogn* 12:83–139.

46. Newman SD, Carpenter PA, Varma S, Just MA (2003): Frontal and parietal participation in problem solving in the Tower of London: fMRI and computational modeling of planning and high-level perception. *Neuropsychologia* 41:1668–1682.

47. Ridderinkhof KR, van den Wildenberg WP, Segalowitz SJ, Carter CS (2004): Neurocognitive mechanisms of cognitive control: The role of prefrontal cortex in action selection, response inhibition, performance monitoring, and reward-based learning. *Brain Cogn* 56:129–140.

48. Friedlander L, Desrocher M (2006): Neuroimaging studies of obsessive-compulsive disorder in adults and children. *Clin Psychol Review* 26:32–49.

49. Insel TR, Winslow JT (1992): Neurobiology of obsessive compulsive disorder. *Psychiatr Clin North Am* 15:813–824.

50. Graybiel AM, Rauch SL (2000): Toward a neurobiology of obsessive-compulsive disorder. *Neuron* 28:343–347.

51. Rosenberg DR, Keshavan MS, Dick EL, Bagwell WW, Macmaster FP, Birmaher B (1997): Corpus callosal morphology in treatment-naive pediatric obsessive compulsive disorder. *Prog Neuropsychopharmacol Biol Psychiatry* 21:1269–1283.

52. Locke S, Angevine JB Jr, Yakovlev PI (1961): Limbic nuclei of thalamus and connections of limbic cortex. II. Thalamocortical projection of the lateral dorsal nucleus in man. *Arch Neurol* 4:355–364.

53. Yakovlev PI, Locke S (1961): Limbic nuclei of thalamus and connections of limbic cortex. III. Corticocortical connections of the anterior cingulate gyrus, the cingulum, and the subcallosal bundle in monkey. *Arch Neurol* 5:364–400.

54. Dillon DG, Pizzagalli DA (2007): Inhibition of action, thought, and emotion: A selective neurobiological review. *Appl Prev Psychol* 12:99–114.

55. Ramnani N, Owen AM (2004): Anterior prefrontal cortex: Insights into function from anatomy and neuroimaging. *Nat Rev Neurosci* 5:184–194.